SUPPLEMENTARY FIGURE LEGENDS

Figure S1. Adipocyte-specific SNAP23 knockout (*AdipSnap23-/-*) mice have increased liver weight with reduced adipose tissue mass. (A) The relative amount of SNAP23 and F4/80 mRNA in epididymal adipose tissue and **(B)** isolated primary adipocytes from 2 to 3-week old *Snap23*$^{fl/fl}$ (WT, filled boxes) and *KO* (KO, open boxes) male mice. These data represent the mean ± SEM from 5 WT and 5 KO mice. **(C)** Primary isolated epididymal adipocytes (4 weeks) from WT, adipocyte-specific heterozygotic (HT) and homozygotic SNAP23 knockout (KO) mice were immunoblotted for SNAP23 and tubulin. The top left panel is light exposure of SNAP23 whereas the right is dark exposure. This is a representative immunoblot performed 2 times. **(D)** Body and tissue weights of several organs from 32-week old male WT and KO mice. These data represent the mean ± SEM from 5 WT and 5 KO mice. **(E)** WT (filled boxes) and KO (open boxes) male mice at 24 weeks of age were subjected to an intraperitoneal glucose tolerance test (GTT). **(F)** Parallel matched mice were subjected to an intraperitoneal insulin tolerance test (ITT). These data represent the mean ± SEM from 4 WT and 4 KO mice. **(G)** Plasma insulin levels were determined from male WT (filled bars) and KO (open bars) following a 5 hrs or 16 hrs fast. This is the mean ± SEM from 8 WT and 5 KO mice. **(H)** Total 24 hrs food intake **(I)** Respiratory exchange rate (RER), **(J)** energy expenditure (EE) and **(K)** spontaneous locomotor activity (AMB+Z) of male WT (filled bars) and KO (open bars). These data represent the mean ± SEM from 4 WT and 6 KO mice. *$p<0.05$ by T tests.

Figure S2. Adipocyte-specific inducible knockdown of SNAP23 in adult mice results in adipocyte cell death in vivo. (A) *Snap23fl/fl* mice were crossed with the tamoxifen inducible *Adipoq-CreERT2*$^{+/-}$ mice to generate *Adipoq-CreERT2*$^{+/-}$ *Snap23fl/fl* mice. At 18 weeks of age, *Adipoq-CreERT2*$^{+/-}$ (IndWT, filled bars) and *Adipoq-CreERT2*$^{+/-}$Snap23fl/fl (IndKO, open bars) male mice were injected daily with tamoxifen over 5 days as described under Experimental Procedures. Five days post tamoxifen injection, isolated epididymal adipocytes was analyzed for mRNA levels of SNAP23 and Beclin 1 by qRT-PCR. These data represent the average with the standard error of the mean from 5 WT and 5 KO mice. **(B)** Epididymal adipose tissue from two representative IndWT (left) and two IndKO (right) mice were fixed, stained with hematoxylin-eosin and examined by light microscopy. **(C)** Epididymal adipose tissue from two representative IndWT (left) and two IndKO (right) mice were fixed and subjected to immunofluorescence microscopy using a perilipin antibody (red) or DAPI stained for nuclei (blue). **(D)** The percentage of perilipin-negative cells was quantified from epididymal adipose tissue. These data were obtained from the counting of 500 cells from 6 IndWT and IndKO mice each and the bar graphs represent the average with the standard error of the mean. **(E)** At 3 weeks of age, subcutaneous adipose tissue stromal vascular cells from *Snap23*$^{fl/fl}$ (WT) and *KO* mice were isolated and cultured. The cells were induced to differentiate as described under Experimental Procedures and images of the cell morphology were taken at day (D) 3, 6, 12 and 15 following addition of the differentiation cocktail. The culture medium was changed every two days over the time frame indicated. These are representative images from 5 independent stromal vascular cell isolations. *$p<0.05$ by T tests.

Figure S3. Starvation in vivo increases adipocyte cell death *in KO* mice. (A) *Snap23*$^{fl/fl}$ (WT) and *KO* male mice at 8 weeks of age where allowed to eat *ad libitum* or starved for 48 hrs. Epididymal adipose tissue were fixed and subjected to immunofluorescence microscopy using a perilipin antibody (red) or DAPI stained for nuclei (blue). Arrows depict areas with multiple nuclei that are perilipin-negative. **(B)** The percentage of perilipin-negative cells was quantified from the epididymal adipose tissue. These data were obtained from the counting of 600 cells from three pairs of WT and KO mice and the bar graphs represent the average with the standard error of the mean. **(C)** The NMshRNA, SNAP23shRNA and rescued SNAP23shRNA/hSNAP23 3T3L1 adipocytes were differentiated in nutrient-replete conditions for 8 days. The cells were then maintained in nutrient-replete or subjected to nutrient-deplete conditions for 2 hrs in the absence and presence of the lysosomotropic agents NH_4Cl and leupeptin. Cell extracts were immunoblotted for p62 and Actin. This is a representative immunoblot independently performed 4 times. **(D)** Quantification of net p62 flux was calculated as the difference between p62 protein levels in the presence and absence of the lysosomotropic agents. **(E, F)** The NMshRNA, SNAP23shRNA and rescued SNAP23shRNA/hSNAP23 3T3L1 adipocytes were differentiated in nutrient-replete conditions for 8 days. The cells were incubated with vehicle (Basal) or 1 μM Isoproterenol (ISO) for 120 min and the amount of released free fatty acid **(E)** or glycerol **(F)** determined. These data represent the mean ± SEM of the mean determined from 3 independent experiments. *p<0.05, ****p<0.0001 by ANOVA with Turkey's test.

Figure S4. SNAP23 deficient NIH3T3 cells results in suppression of autophagy and induction of nutrient-dependent cell death. (A) NMshRNA and SNAP23shRNA NIH3T3 cells grown under nutrient replete (NR) conditions were treated with nutrient deplete (ND) medium for 2 hrs in the absence and presence of NH_4Cl and leupeptin. Cell extracts were immunoblotted for LC3, Actin and SNAP23. **(B)** Quantification of net LC3-II flux was calculated and these data represent the mean ± SEM from 4 independent experiments. **(C)** NMshRNA and SNAP23shRNA NIH3T3 cells grown under NR conditions were incubated with ND medium for 2 hrs in the absence and presence of NH_4Cl and leupeptin. Cell extracts were prepared and immunoblotted for p62 and Actin. **(D)** Quantification of net p62 flux was calculated and these data represent the mean ± SEM from 4 independent experiments. **(E)** The NMshRNA and SNAP23shRNA NIH3T3 cells were then maintained under NR or ND conditions for 6 h and subjected to propidium iodide (PI) and DAPI labeling. Scale bars: 100 μm. **(F)** Quantification of the PI positive nuclei was determined by the counting of 1000 cells per group from 3 independent determinations. These data represent the mean ± SEM from 3 independent experiments. **(G)** The presence of oligonuclesome in cytoplasmic lysates from NMshRNA and SNAP23shRNA NIH3T3 cells maintained under NR or ND conditions for 6 h. The fold increase is presented relative to the NMshRNA cells in the nutrient replete state. These data represent the mean ± SEM from 3 independent experiments. *$p<0.05$, **$p<0.01$, ***$p<0.001$, ****$p<0.0001$ by T tests (B and D) or by ANOVA with Turkey's test (F and G).

Figure S5. SNAP23 deficiency in vivo suppresses the number of adipocyte autophagosomes. Interscapular brown adipose tissue from *Snap23*$^{fl/fl}$ (WT) and *KO* male mice at 2 weeks of age were dissected, fixed, embedded and thin sections prepared for transmission electron microscopy as described under Experimental Procedures. **(A)** Three representative low magnification and three high magnification field sections from *Snap23*$^{fl/fl}$ (WT) brown adipose tissue are shown. Three representative low magnification and three high magnification field sections from *KO* brown adipose tissue are shown. Mitochondria are labeled with an m, lipid droplets with LD and autophagosomes are indicated with the black arrows. **(B)** The number of autophagosomes was quantified by counting the number of double membrane structures in 17 images of the *Snap23*$^{fl/fl}$ (WT) and 18 images of the *KO* brown adipocytes. **(C)** NMshRNA and SNAP23shRNA NIH3T3 cells in duplicate were maintained under nutrient replete medium and or nutrient depleted for 1 hr. Cell extracts were then immunoblotted for ULK1-S555, ULK1, AMPK-T172 and total AMPK. These are representative immunoblots from 4 independent experiments. **(D)** Quantification of LC3-II flux from NMshRNA and SNAP23shRNA cells with and without BAX siRNA knockdown was calculated as the difference between LC3-II protein levels in the presence and absence of the lysosomotropic agents. These data represent the mean ± SEM determined from 3 independent experiments. *P<0.05 by T tests **(B)** and ANOVA with Turkey's test **(D)**.

Figure S6. BAX protein is elevated and BAX deficiency rescues the loss of adipose tissue in the *KO* mice. (A) The NMshRNA and SNAP23shRNA NIH3T3 cells

were then maintained under nutrient replete conditions and cell extracts were prepared and immunoblotted for SNAP23, BAX, Bcl-xL, Mcl-1, Bcl-2, BAK and Actin. The immunoblots for Bcl-2 and BAK are from same samples run on parallel gels. These are representative immunoblots from 3 independent experiments of two cell lines each. **(B)** Interscapular brown adipose tissue (iBAT) an epididymal white adipose tissue (Epi) was isolated from 4-5 weeks old *Snap23*$^{fl/fl}$ (WT) and *KO* mice and tissue extract were immunoblotted for BAX and tubulin. The specificity for the BAX antibody was demonstrated by inclusion of adipose tissue extracts from BAX knockout mice (BAX$^{-/-}$). **(C)** Represent images of Interscapular brown (BAT), epididymal (Epi) and subcutaneous (Sub) adipose tissue from 4-5 weeks old male *Snap23*$^{fl/fl}$ (WT) and *KO* and *KO*/BAX$^{+/-}$ mice. **(D)** The tissue weights of the genotypes indicated from 5 male mice were quantified. **(E)** Non-targeted, ATG9sgRNA (ATG9KO) and rescued (ATG9KO/hAT9) NIH3T3 cells were maintained under nutrient replete conditions, the cell extracts were then immunoblotted for BAX and Actin. These are representative immunoblots independently performed 4 times. **(F)** Non-targeted, ATG9sgRNA (ATG9KO) and rescued (ATG9KO/hAT9) NIH3T3 cells were maintained under nutrient replete conditions and treated with the lysosomotropic agents, the cell extracts were immunoblotted for LC3 and Actin. (**G)** Quantitated net LC3-II flux in non-targeted, ATG9sgRNA (ATG9KO) and rescued (ATG9KO/hAT9) NIH3T3 cells. **(H)** The NMshRNA and SNAP23shRNA NIH3T3 cells in duplicate were transfected with NSsiRNA or BAXsiRNA for 48 hrs then proteins were extracted for ATG9 and Actin immunoblotting. The Actin immunoblot is from same samples run on a parallel gel.

These data are representative from three independent experiments. $p<0.05$, $^{**}p<0.01$ by ANOVA with Turkey's tests.

Figure S7. BAX associates with LC3 positive autophagic vacuoles. (A) NIH3T3 cells were co-transfected with cDNAs encoding HA-BAX and GFP-LC3 and maintained under nutrient replete conditions. Twenty-four h later, the cells were placed in nutrient deplete (ND) media for 1 hr in the absence (panels 1-3) and presence (panels 4-6) of the lysosomotropic agents. The cells were then visualized by fluorescence microscopy. Scale bars: 15 μm and 7.5 μm (insert). **(B)** The extent of puncta co-localized HA-BAX and GFP-LC3 was determined by Pearson's coefficient from 5 independent experiments with the quantification from 50 cells/experiment. **(C)** Mitophagy was analyzed by double immunostaining for TOM20 (green) and LAMP1 (red) with DAPI (blue) labeling of the nuclei. These pictures are representative of 50 cells for each treatment. Scale bars: 7.5 μm and 2.5 μm (insert). **(D)** Mitophagy was analyzed by immunoblotting TOM20 under nutrient replete (NR) and nutrient deplete (ND) condition in the absence and presence of lysosomotropic agents, NH_4Cl and leupeptin. These data are representative of three independent experiments. **(E)** Quantification of TOM20 flux was calculated as the difference between TOM20 protein levels in the presence and absence of the lysosomotropic agents. These data represent the mean ± SEM determined from 3 independent experiments. $^{**}p<0.01$ by T tests.

Figure S8. SNAP23 and ATG9 deficiency has no effect on transferrin receptor plasma membrane endocytosis. (A) Control NMshRNA, SNAP23shRNA and

ATG9KO NIH3T3 cells were treated with vehicle (lanes 1-3) or 80 μM dynasore (lanes 4-6) for 30 min under nutrient deplete conditions and then incubated with Alexa Fluor 594-transferrin for 10 min at 37^{o}C. Cells were washed with isotonic acidic buffer (0.5M glycine, pH 2.8) followed by neutral buffer (PBS, pH 7.0) at 4^{o}C. Cells were fixed and visualized by fluorescence microscopy. These are representative images from 5 independent determinations. Scale bars: 25 μm. **(B)** At 3 weeks of age, subcutaneous adipose tissue stromal vascular cells from WT and KO mice were isolated, differentiated (4 days) and subjected to the Alexa Fluor 594-transferrin endocytosis protocol as described in **(A)**. Cells were fixed and visualized by fluorescence microscopy. These are representative images from 3 independent determinations. Scale bars: 25 μm. **(C)** NMshRNA and SNAP23shRNA 3T3L1 cells were treated with vehicle or 100 nM insulin for 30 min followed by the addition of 2-[^{3}H] deoxyglucose for 30 min. These data represent the mean ± SEM from 3 independent experiments. **(D)** 3T3L1 adipocytes were co-transfected SNAP23 siRNAs and HA-GLUT4-GFP for 48 hrs. The cells were treated with the indicated concentrations of insulin and the ratio of exofacial HA labeling versus total GFP signal was quantified. These data represent the mean ± SEM from 3 independent experiments. **(E)** Cell extracts were isolated and immunoblotted for SNAP23 and actin. **(F)** The NMshRNA and SNAP23shRNA NIH3T3 cells were maintained under NR or ND conditions for 1 or 3 hrs and loaded with Fluo-8 for 30 min. The cytosolic calcium levels were normalized to protein concentration. These are the average of 3 independent determinations with mean ± SEM. ****$p<0.0001$ by ANOVA with Turkey's test.

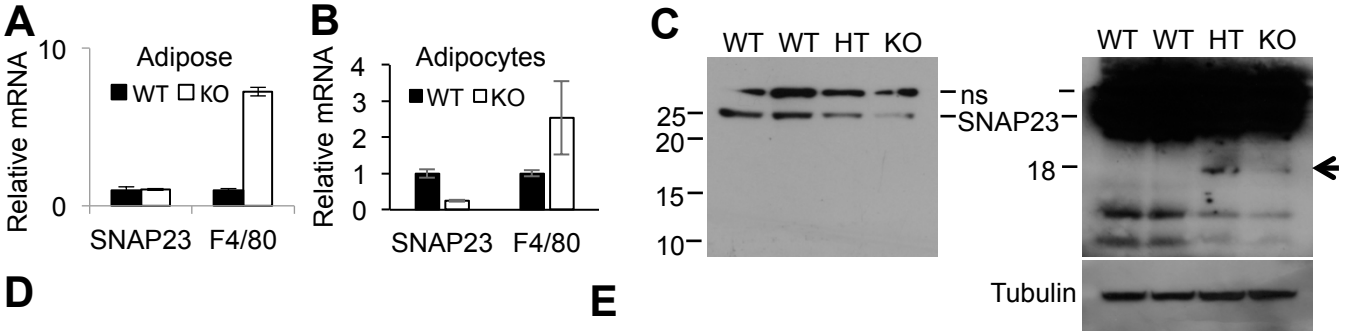

D

Body and tissue weight (g) of KO mice.

	WT	KO
Body weight	32.52±1.64	41.55±3.02*
Liver	1.18±0.10	5.54±1.03**
EPI	0.95±0.26	0±0*
SUB	0.42±0.10	0±0 *
Perirenal	0.26±0.06	0±0 *
BAT	0.09±0.004	0±0 *
Pancreas	0.21±0.01	0.33±0.03**
Heart	0.16±0.02	0.21±0.01
Lung	0.18±0.01	0.21±0.01*
Gastrocnemius	0.34±0.04	0.32±0.003
Brain	3.8±0.06	4.59±0.25**
Intestine	3.26±0.28	4.83±0.27**
Seminal vesicle	0.92±0.34	5.26±1.12**
Kidney	0.46±0.02	0.62±0.05*

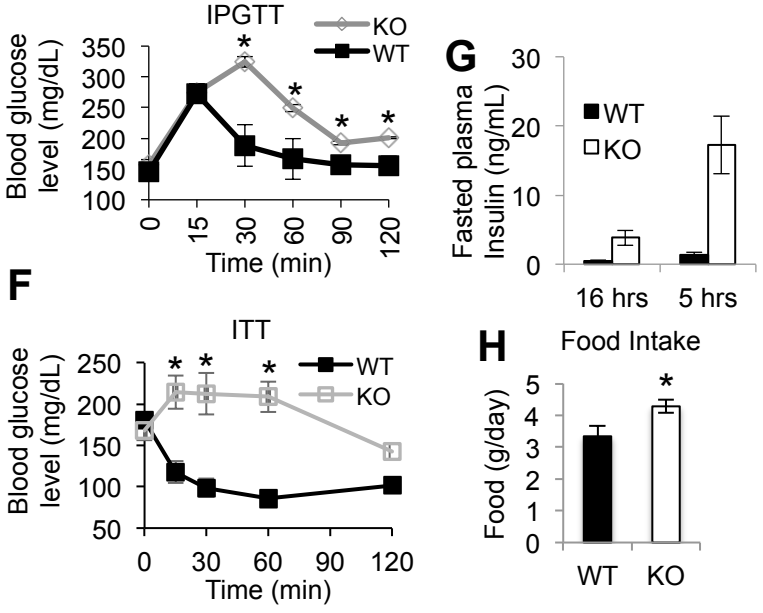

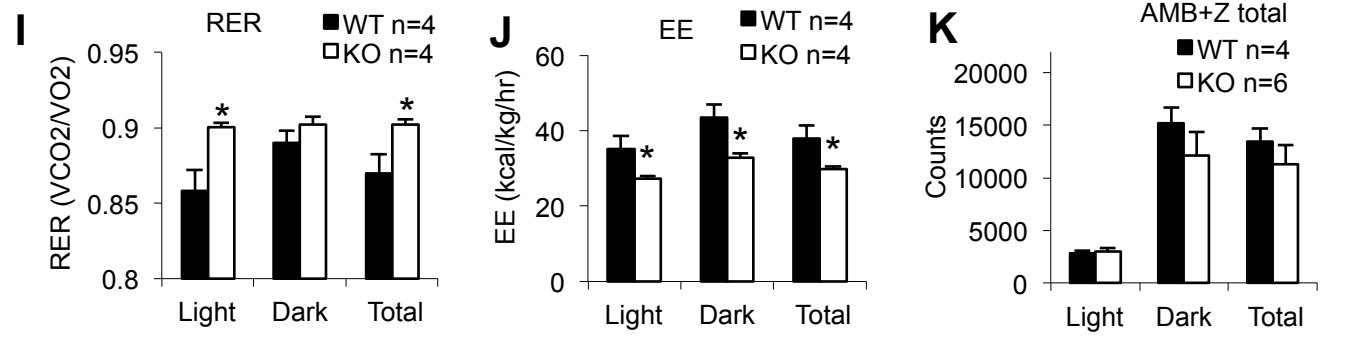

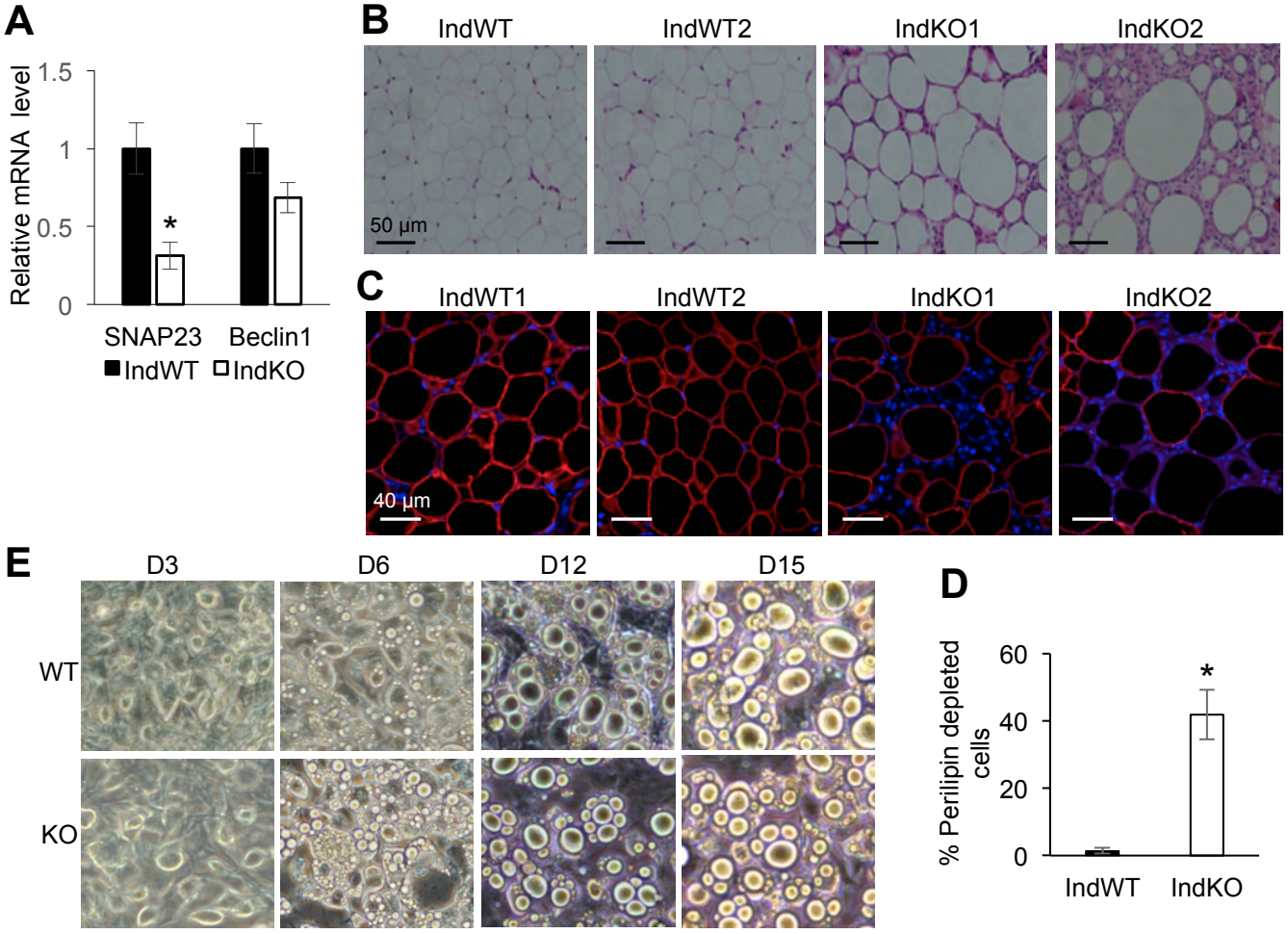
A
Relative mRNA level
1.5
1
0.5
0
*
SNAP23
Beclin1
IndWT
IndKO
B
IndWT
IndWT2
IndKO1
IndKO2
50 μm
C
IndWT1
IndWT2
IndKO1
IndKO2
40 μm
E
D3
D6
D12
D15
WT
KO
D
% Perilipin depleted cells
60
40
20
0
*
IndWT
IndKO

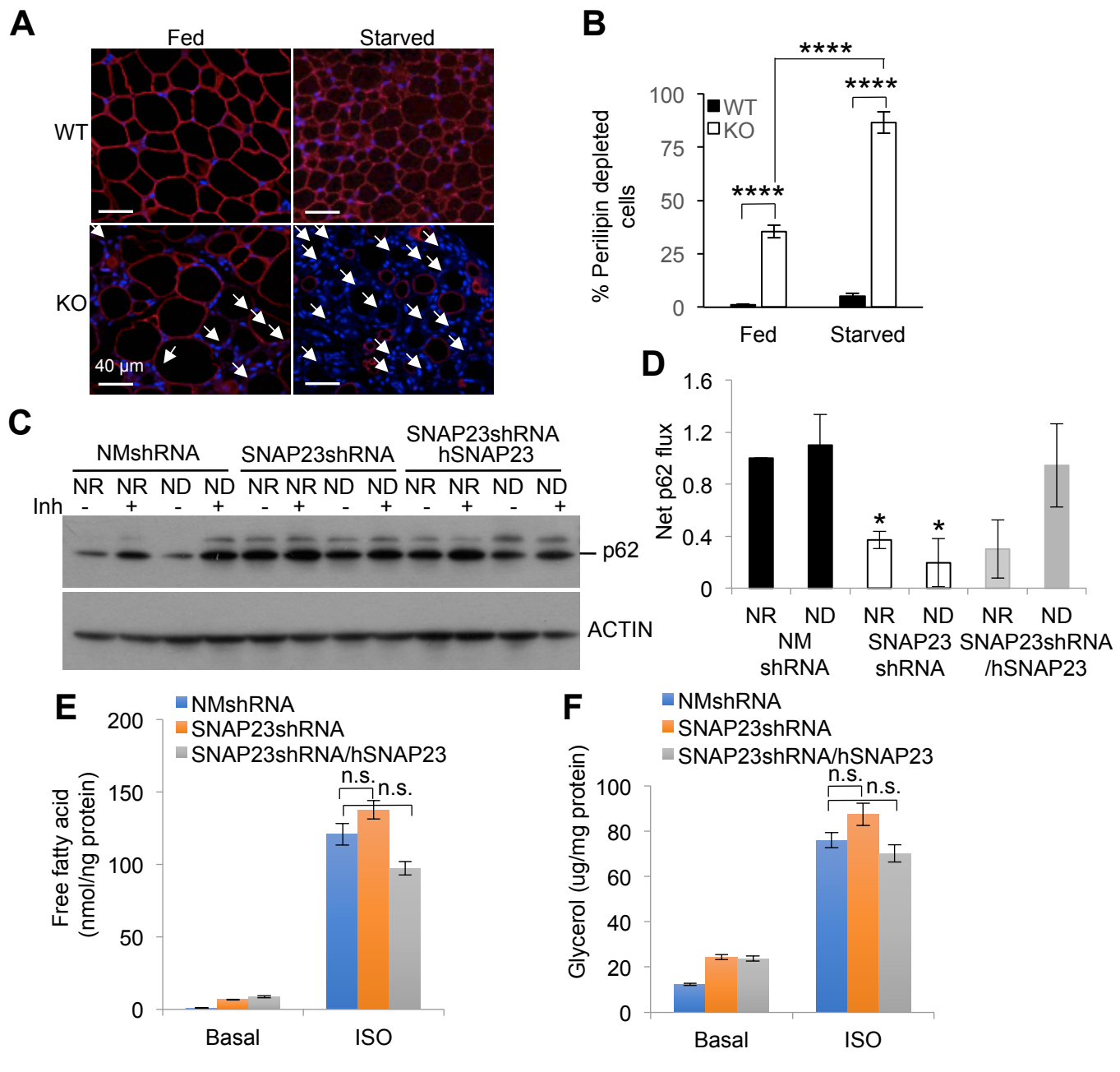
A
Fed
Starved
WT
KO
40 μm
B
% Perilipin depleted cells
WT
KO
****
****
****
100
75
50
25
0
Fed
Starved
C
NMshRNA
SNAP23shRNA
SNAP23shRNA hSNAP23
NR NR ND ND NR NR ND ND NR NR ND ND
Inh - + - + - + - + - + - +
p62
ACTIN
D
Net p62 flux
1.6
1.2
0.8
0.4
0
*
*
NR ND NR ND NR ND
NM shRNA
SNAP23 shRNA
SNAP23shRNA /hSNAP23
E
NMshRNA
SNAP23shRNA
SNAP23shRNA/hSNAP23
Free fatty acid (nmol/ng protein)
200
150
100
50
0
n.s.
n.s.
Basal
ISO
F
NMshRNA
SNAP23shRNA
SNAP23shRNA/hSNAP23
Glycerol (ug/mg protein)
100
80
60
40
20
0
n.s.
n.s.
Basal
ISO

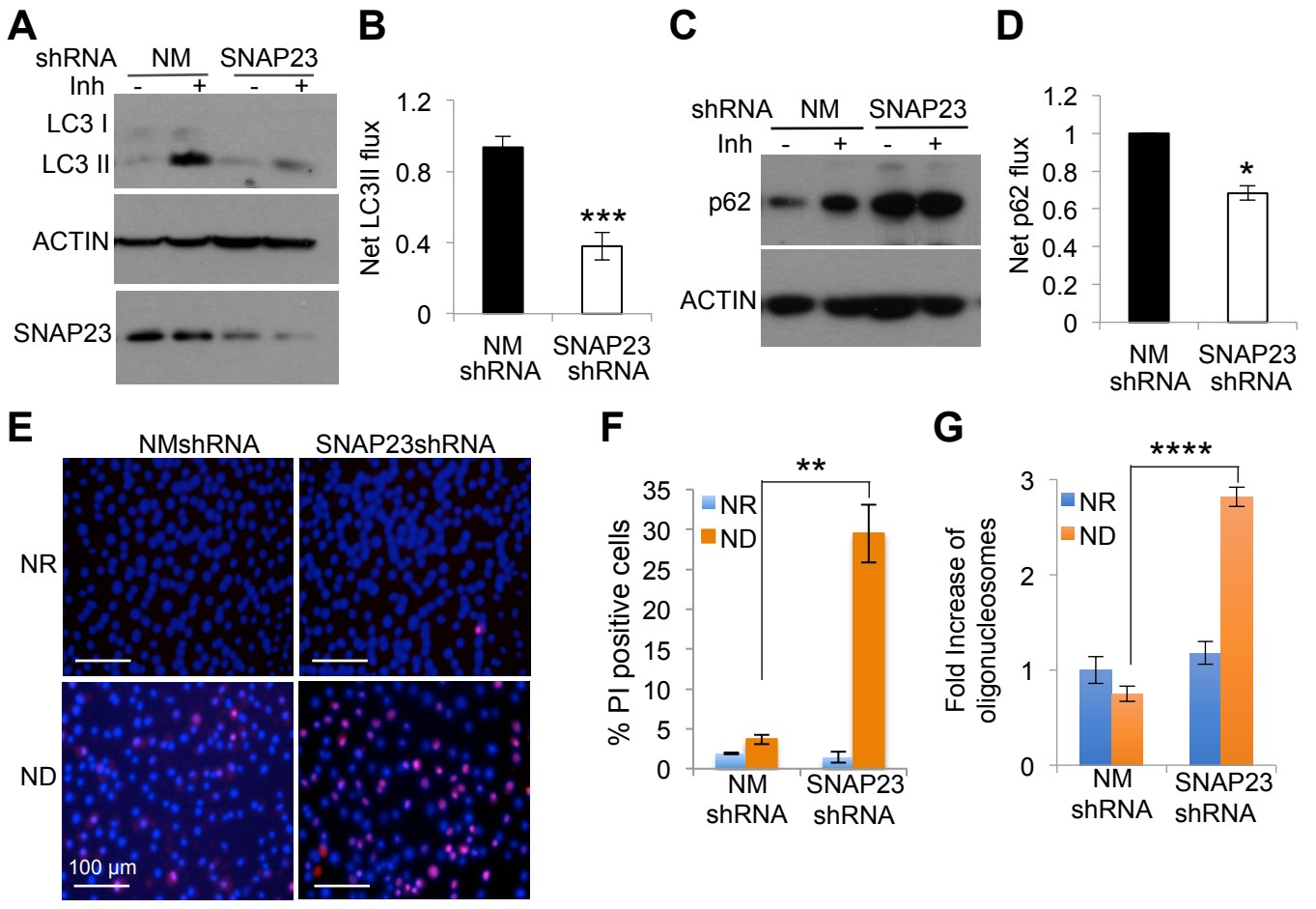
A
shRNA
NM
SNAP23
Inh
-
+
-
+
LC3 I
LC3 II
ACTIN
SNAP23
B
Net LC3II flux
1.2
0.8
0.4
0
***
NM shRNA
SNAP23 shRNA
C
shRNA
NM
SNAP23
Inh
-
+
-
+
p62
ACTIN
D
Net p62 flux
1.2
1
0.8
0.6
0.4
0.2
0
*
NM shRNA
SNAP23 shRNA
E
NMshRNA
SNAP23shRNA
NR
ND
100 µm
F
% PI positive cells
35
30
25
20
15
10
5
0
**
NR
ND
NM shRNA
SNAP23 shRNA
G
Fold Increase of oligonucleosomes
3
2
1
0
****
NR
ND
NM shRNA
SNAP23 shRNA

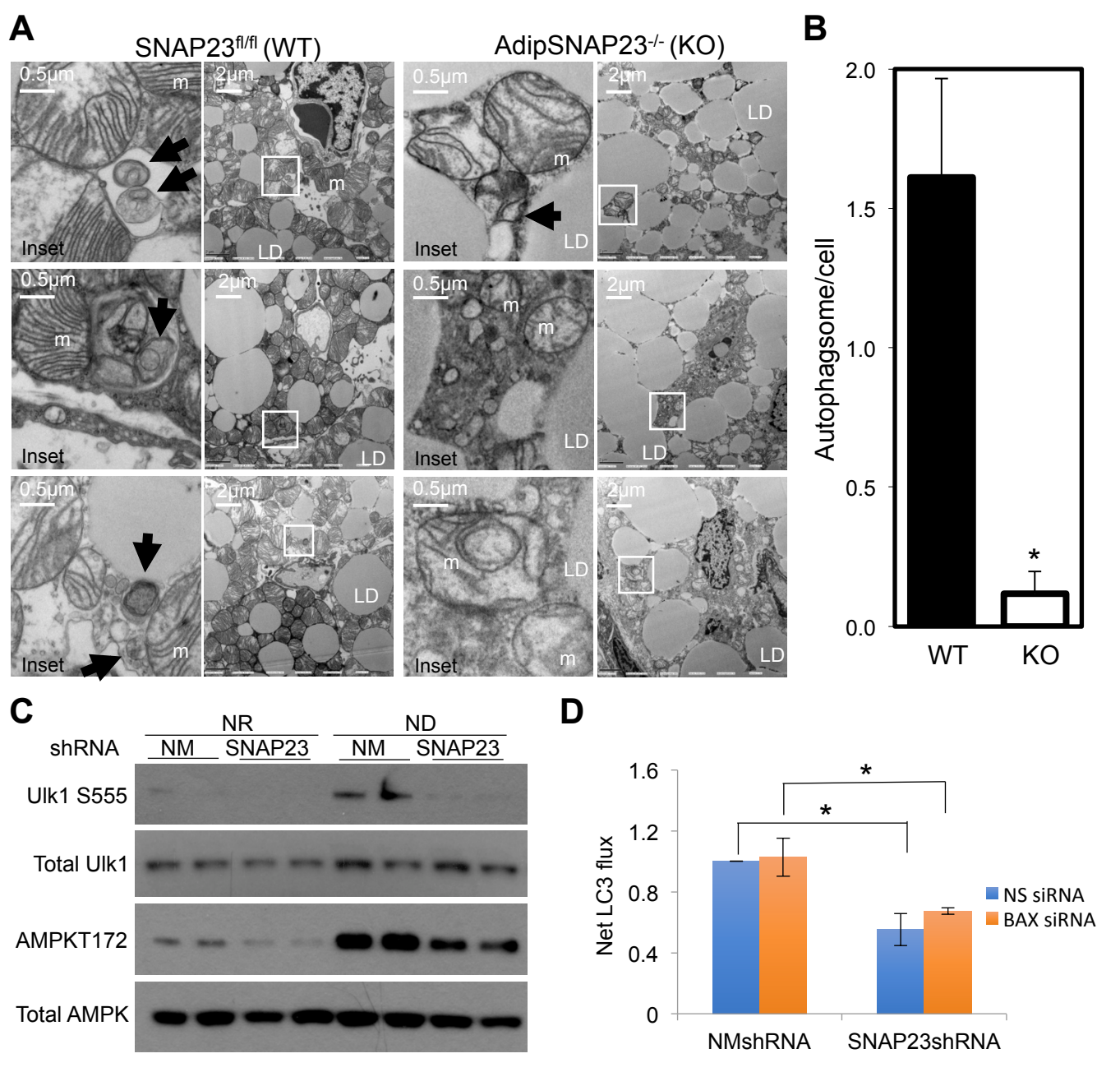
A
SNAP23fl/fl (WT)
AdipSNAP23-/- (KO)
0.5μm
2μm
m
LD
Inset
B
Autophagsome/cell
2.0
1.5
1.0
0.5
0.0
*
WT
KO
C
NR
ND
shRNA
NM
SNAP23
NM
SNAP23
Ulk1 S555
Total Ulk1
AMPKT172
Total AMPK
D
Net LC3 flux
1.6
1.2
0.8
0.4
0
*
*
NS siRNA
BAX siRNA
NMshRNA
SNAP23shRNA

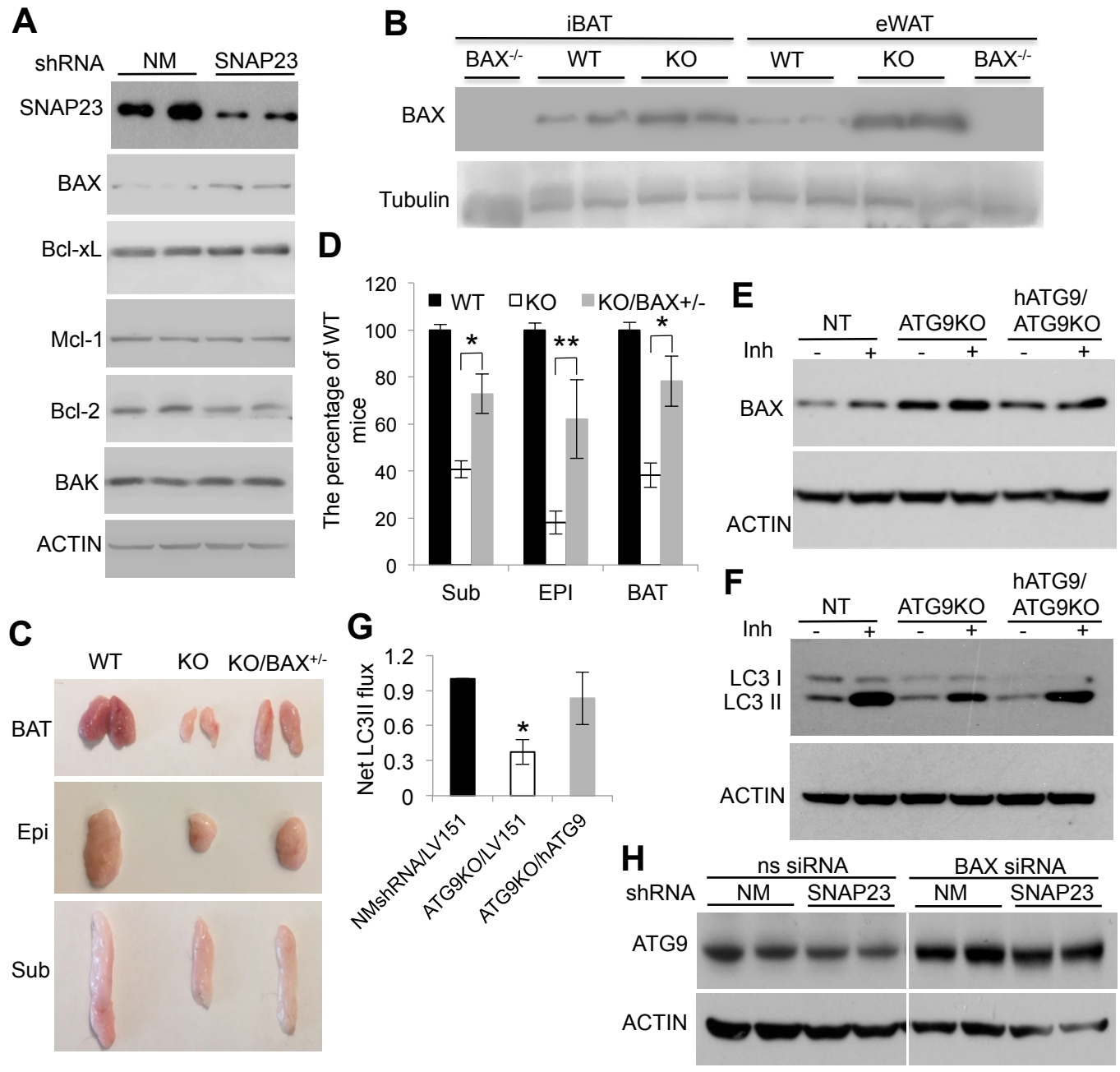
A
shRNA
NM
SNAP23
SNAP23
BAX
Bcl-xL
Mcl-1
Bcl-2
BAK
ACTIN
B
iBAT
eWAT
BAX-/-
WT
KO
WT
KO
BAX-/-
BAX
Tubulin
C
WT
KO
KO/BAX+/-
BAT
Epi
Sub
D
WT
KO
KO/BAX+/-
The percentage of WT mice
120
100
80
60
40
20
0
*
**
*
Sub
EPI
BAT
E
NT
ATG9KO
hATG9/ ATG9KO
Inh
- + - + - +
BAX
ACTIN
F
NT
ATG9KO
hATG9/ ATG9KO
Inh
- + - + - +
LC3 I
LC3 II
ACTIN
G
Net LC3II flux
1.2
0.9
0.6
0.3
0
*
NMshRNA/LV151
ATG9KO/LV151
ATG9KO/hATG9
H
ns siRNA
BAX siRNA
shRNA
NM
SNAP23
NM
SNAP23
ATG9
ACTIN

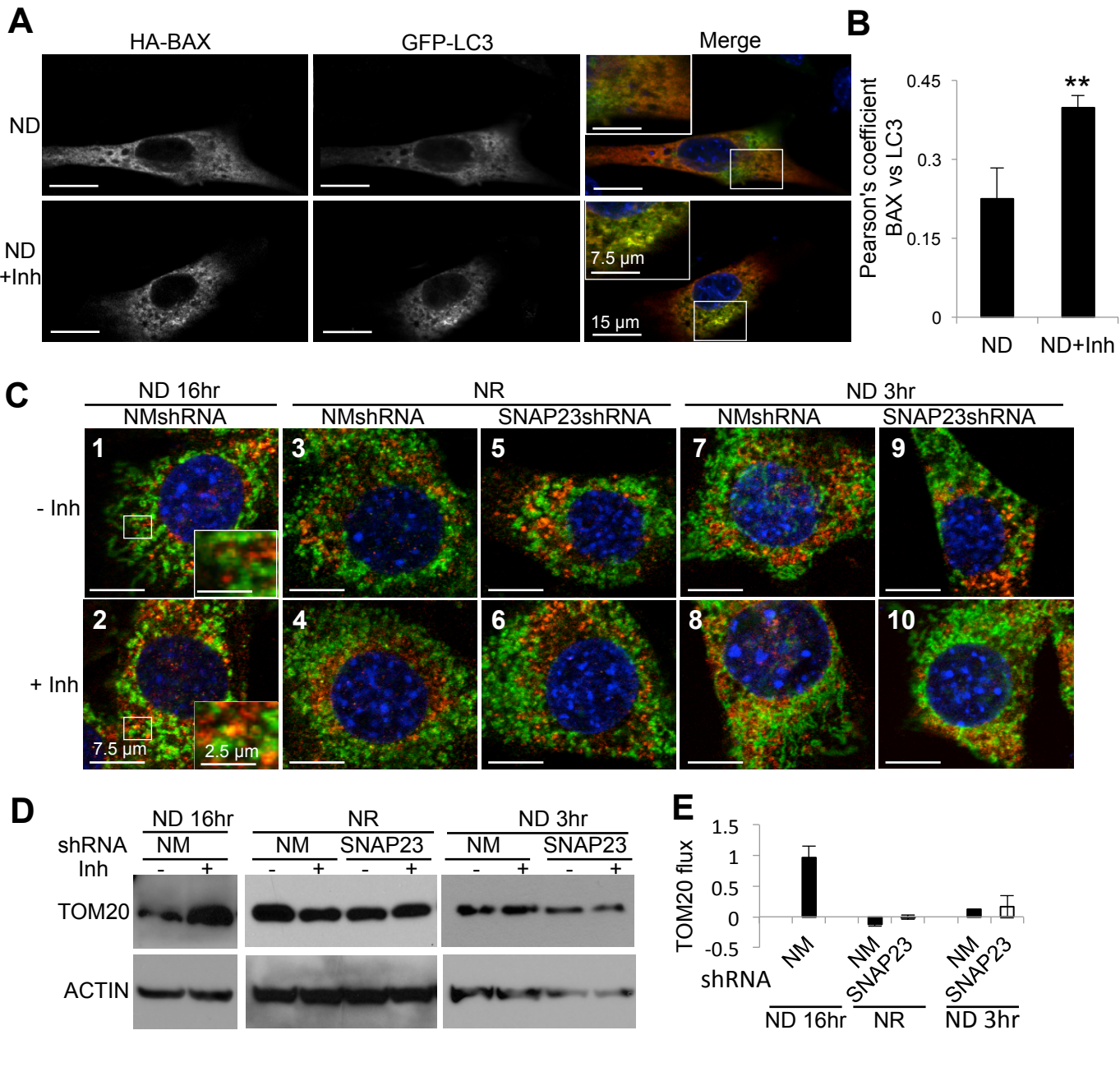
A
HA-BAX
GFP-LC3
Merge
ND
ND +Inh
7.5 µm
15 µm
B
Pearson's coefficient BAX vs LC3
0.45
0.3
0.15
0
**
ND
ND+Inh
C
ND 16hr
NR
ND 3hr
NMshRNA
NMshRNA
SNAP23shRNA
NMshRNA
SNAP23shRNA
- Inh
+ Inh
1
2
3
4
5
6
7
8
9
10
7.5 µm
2.5 µm
D
ND 16hr
NR
ND 3hr
shRNA
NM
NM
SNAP23
NM
SNAP23
Inh
- + - + - + - + - +
TOM20
ACTIN
E
TOM20 flux
1.5
1
0.5
0
-0.5
shRNA
NM
NM
SNAP23
NM
SNAP23
ND 16hr
NR
ND 3hr

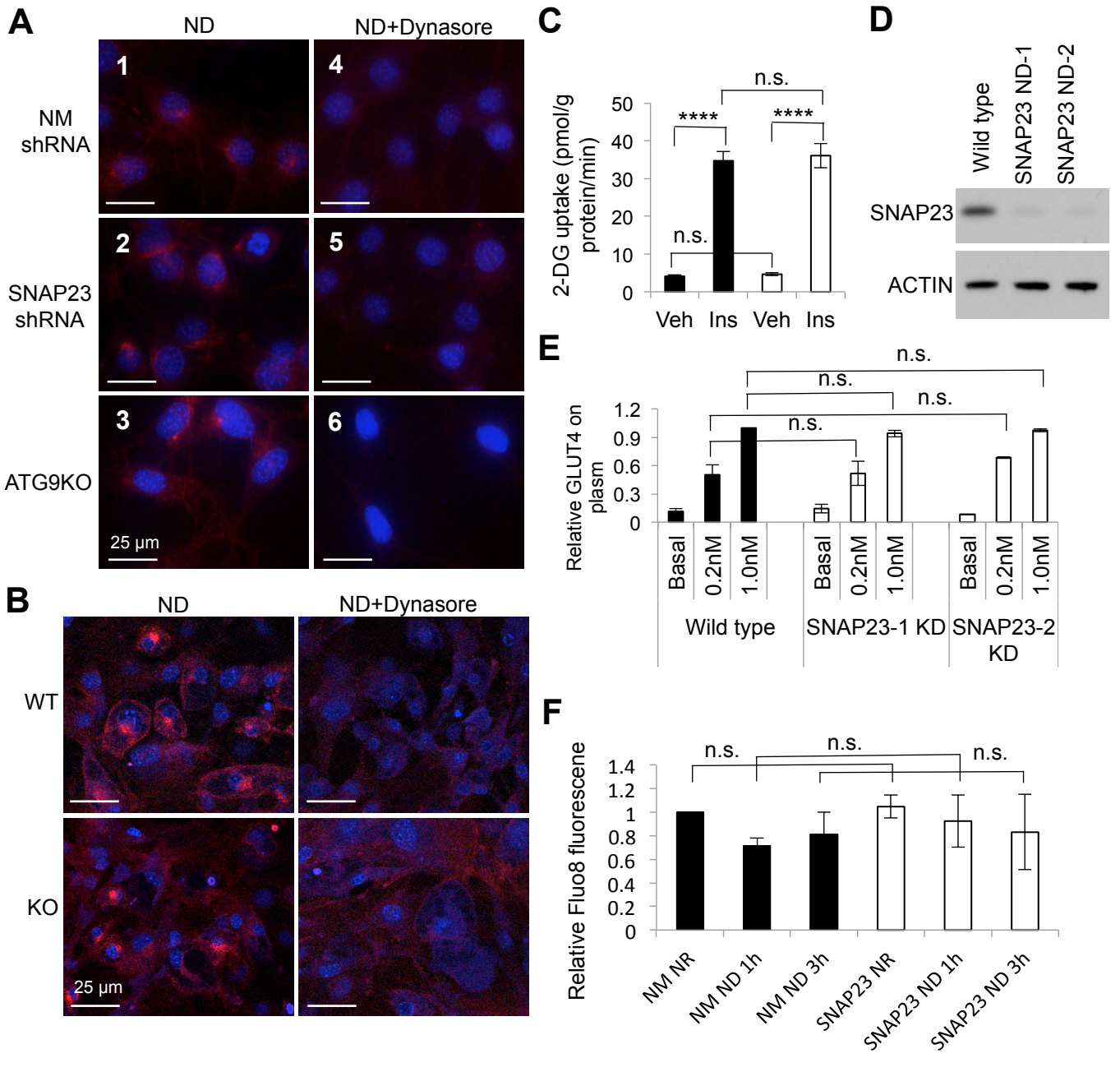
A
ND
ND+Dynasore
NM shRNA
SNAP23 shRNA
ATG9KO
1
2
3
4
5
6
25 μm
B
ND
ND+Dynasore
WT
KO
25 μm
C
2-DG uptake (pmol/g protein/min)
50
40
30
20
10
0
n.s.
****
****
n.s.
Veh
Ins
Veh
Ins
D
Wild type
SNAP23 ND-1
SNAP23 ND-2
SNAP23
ACTIN
E
Relative GLUT4 on plasm
1.2
0.9
0.6
0.3
0
n.s.
n.s.
n.s.
n.s.
Basal
0.2nM
1.0nM
Basal
0.2nM
1.0nM
Basal
0.2nM
1.0nM
Wild type
SNAP23-1 KD
SNAP23-2 KD
F
Relative Fluo8 fluorescene
1.4
1.2
1
0.8
0.6
0.4
0.2
0
n.s.
n.s.
n.s.
NM NR
NM ND 1h
NM ND 3h
SNAP23 NR
SNAP23 ND 1h
SNAP23 ND 3h